

PONTIFICIA UNIVERSIDAD CATÓLICA DEL PERÚ

ESCUELA DE POSGRADO



Experimental research of extended polarization coherence theorem for nonclassical light

Tesis para optar el grado de Magíster en Física que presenta

Max Jara Ortiz

Asesor:

Francisco Antonio De Zela Martinez

Lima, 2023

Informe de Similitud

Yo, ...Francisco De Zela....., docente de la Escuela de Posgrado de la Pontificia Universidad Católica del Perú, asesor de la tesis/el trabajo de investigación titulado Experimental research of extended polarization coherence theorem for nonclassical light....., del autor

.....
Max Jara Ortíz.....,
.....,
.....,

dejo constancia de lo siguiente:

- El mencionado documento tiene un índice de puntuación de similitud de 11%. Así lo consigna el reporte de similitud emitido por el software *Turnitin* el 26/04/2023.
- He revisado con detalle dicho reporte y la Tesis o Trabajo de Suficiencia Profesional, y no se advierte indicios de plagio.
- Las citas a otros autores y sus respectivas referencias cumplen con las pautas académicas.

Lugar y fecha:

Lima, 26 de abril de 2023.....

Apellidos y nombres del asesor / de la asesora: <u>De Zela Martínez Francisco Antonio</u>	
DNI:10540939	Firma <i>Francisco De Zela</i>
ORCID:0000-0002-3757-1769	

Resumen

Esta tesis reporta la demostración experimental de una extensión del teorema de la coherencia de polarización (PCT), un teorema que estableció una restricción entre la distinguibilidad y la visibilidad, dos cantidades que sirven, respectivamente, como medida de el comportamiento de el tipo partícula y de el tipo onda los cuales pueden aparecer simultáneamente en los arreglos interferométricos. Si bien el PCT se aplica tanto en el régimen cuántico como en el clásico, esta tesis se centra en el caso cuántico. Los experimentos se llevaron a cabo con fotones individuales. La extensión teórica de la PCT que se sometió a prueba experimental es mucho mas complicada que la PCT original y planteó varios retos técnicos. Esta tesis informa de la exitosa realización de los experimentos. Las técnicas utilizadas también podrían emplearse, con ligeras modificaciones, al trabajar con luz clásica. El marco general, al que contribuyen nuestros resultados, se refiere a la llamada dualidad onda-partícula y al principio de complementariedad de Bohr. Este es un tema de intensa investigación que aborda no solo cuestiones fundamentales de la mecánica cuántica, sino también aplicaciones prácticas en la ciencia de la información cuántica.

Abstract

This thesis reports the experimental display of an extension of the polarization coherence theorem (PCT), a theorem that established a constraint between distinguishability and visibility, two quantities that serve, respectively, as a measure of particle-like and wave-like behavior that may simultaneously appear in interferometric arrangements. While the PCT applies in both quantum and classical regimes, this thesis focuses on the quantum case. The experiments were conducted using single photons. The theoretical extension of the PCT that was submitted to experimental test is much more involved than the original PCT and put several technical challenges. This thesis reports the successful implementation of the experiments. The techniques used could also be employed, with slight modifications, when working with classical light. The general framework, in which our results make a contribution, refers to so-called wave-particle duality and Bohr's complementarity principle. This is a topic of intensive research that addresses not only foundational issues in quantum mechanics but also practical applications in quantum information science.

Acknowledgements

This thesis is in some way the result of a conjunction of favorable circumstances as family support, professor mentoring, friendship of lab members and a big effort to achieve the experimental goal. My mother Agustina, my father Máximo and my brothers Diego, Edison and Liz have been a constant support without which this work would have taken considerably longer. I really thank to my family to help me in every difficult moments and for accompanying to make the days more bearable during the process of this thesis. I really appreciate the mentoring of Professor Francisco de Zela for his classes and advices to let me develop my experimental and theoretical skills in the laboratory as proposing new ideas. The environment in the laboratory of give each student freedom in the Quantum Optics group is the cause I was fullfully gratified to be more creative. I would also like to thank Professor Eduardo Massoni and Hernan Castillo for giving me consultancies and receive my own ideas. My friends have certainly played an important part too. Carlos, Joel and Victor, thanks for your unconditional friendship during these two years. I also thank Yonny, Jean Paul and David for the shared advices in the lab during the measurements. I thank all the people not mentioned but had impact on this work.

Contents

Resumen	i
Abstract	ii
Acknowledgements	iii
Contents	iv
1 Preliminary concepts	1
1.1 Two-state systems	1
1.1.1 Hilbert space	1
1.1.2 Qubit	2
1.2 Path and polarization qubits	4
1.2.1 Polarization qubit	4
1.2.2 Path and polarization qubits	6
1.3 Mixed states for polarization and path qubits	7
1.4 Extended polarization coherence theorem	11
2 Experimental arrangements	13
2.1 Generation of path states and mixed polarization states	13
2.1.1 Generation of path states	13
2.1.2 Generation of mixed polarization states	14
2.2 Experimental setup	16
2.3 Technical information and experimental details	20
2.3.1 Technical information	20
2.3.2 Experimental details	21
3 Results	23
3.1 Measurement of visibility	23
3.1.1 Pure polarized states	24
3.1.2 Partially polarized states	26
3.1.3 Non polarized states	27

3.2	Measurement of distinguishability	28
3.2.1	Pure polarized states	30
3.2.2	Partially polarized state	32
3.2.3	Non polarized state	33
3.3	The sum of visibility and distinguishability squared	34
3.3.1	Pure polarized state	35
3.3.2	Partially polarized state	36
3.3.3	Non polarized state	37
4	Summary	39
	Bibliography	41



Chapter 1

Preliminary concepts

In this chapter, basic concepts will be presented to support the formalism behind the experimental research. The definitions of Hilbert space, two-state systems, mixed states for polarization and path qubits and the polarization coherence theorem (PCT) establish the basis of the present thesis.

1.1 Two-state systems

1.1.1 Hilbert space

The vector space in which all quantum states lie is a Hilbert space. Formally, a Hilbert space is an inner-product space V which is a Banach space with respect to the induced norm [1]. If V is an inner product space, it maps $(\cdot, \cdot) : V \times V \rightarrow \mathbb{C}$ satisfying the conditions of Hermitian symmetry, linearity and positive definiteness. These conditions are shown below, in the same

order:

$$\begin{aligned}(x, y) &= \overline{(y, x)} \quad \forall x, y \in V \\ (\alpha x_1 + \beta x_2, y) &= \alpha(x_1, y) + \beta(x_2, y) \quad \forall x_1, x_2, y \in V, \alpha, \beta \in \mathbb{C} \\ (x, x) &\geq 0 \text{ and } (x, x) = 0 \Leftrightarrow x = 0 \quad \forall x \in V.\end{aligned}\tag{1.1}$$

It is possible to induce a norm $\|\cdot\|$ in V with inner product (\cdot, \cdot) , as follows:

$$\|x\| = \sqrt{(x, x)} \quad \forall x \in V.\tag{1.2}$$

Finally, the Hilbert space is a Banach space if every Cauchy sequence x_i of vectors converges to some vector x in that space. For simplicity, we will use a finite dimensional Hilbert space \mathbb{C}^n . In particular, the subspace \mathbb{C}^2 allows to define a two-state system \mathcal{H}_2 .

1.1.2 Qubit

Classical physics was not successful in predicting the result of the Stern-Gerlach experiment. This experiment sheds lights on the nature of spin states, some of which might seem counterintuitive. A setup of three Stern-Gerlach devices and filters allow to make evident that, e.g., spin up in +z direction is a superposition of spin up and spin down states on the x direction and vice versa. This holds for any two-state system [2]. In addition, many other physical entities have the same property of quantum superposition. Under realistic conditions, there is a finite time of coherence, i.e., a finite duration of the quantum superposition property. It is useful to define a mathematical object that represents the superposition of two states. This is the quantum bit or qubit.

In classical information and classical computation, the bit is the fundamental unit. It can take on two values, 0 and 1. In contrast to a classical bit, a qubit has a variety of possible states, because superposition is its primary feature.

A general qubit will be built as a superposition of states. The orthonormal basis $\{|0\rangle, |1\rangle\}$ and the $\alpha, \beta \in \mathbb{C}$ coefficients define a general state on a two-state system as

$$|\psi\rangle = \alpha |0\rangle + \beta |1\rangle, \quad (1.3)$$

where $|\psi\rangle \in \mathcal{H}_2$.

From a different angle, a geometric representation of a qubit can be visualized on a unit sphere S^2 . Given the state

$$|\psi\rangle = \cos \frac{\theta}{2} |0\rangle + e^{i\varphi} \sin \frac{\theta}{2} |1\rangle, \quad (1.4)$$

where $\theta, \varphi \in \mathbb{R}$, it defines a point or a vector, with unit length, on the surface of the sphere shown in Fig. 1.1

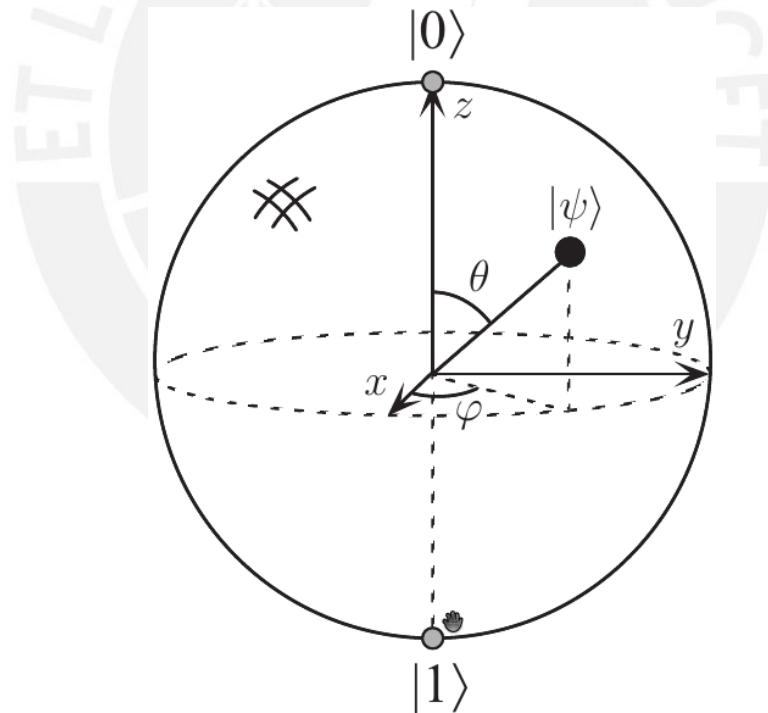


Figure 1.1: Bloch sphere and qubit representation.

In quantum computing this sphere is named Bloch sphere and it is used on the context of a two-state system for representing pure states.

1.2 Path and polarization qubits

1.2.1 Polarization qubit

Polarized states are two-state systems. The description of polarization is given in terms of the electric field of paraxial beams or single photon beams. This field corresponds to a plane wave and can be given in terms of two orthogonal polarization vectors, which are also orthogonal to the wave vector, the vector that points along the beam. A general electric field can be written as

$$\mathbf{E}(r, t) = \frac{i}{\epsilon_0^{1/2} L^{3/2}} \sum_{\mathbf{k}} \sum_s \omega_k [u_{\mathbf{k}s}(t) \boldsymbol{\epsilon}_{\mathbf{k},s} e^{i\mathbf{k}\cdot\mathbf{r}} - \text{c.c.}], \quad (1.5)$$

where the angular frequency is $\omega_{\mathbf{k}} = ck$, the mode amplitude is $u_{\mathbf{k}s}(t)$ and the polarization vector is $\boldsymbol{\epsilon}_{\mathbf{k},s}$ with $s = 1, 2$.

In light of the aforementioned description of electric field, it is convenient to choose

$$\mathbf{k} \cdot \boldsymbol{\epsilon}_{\mathbf{k},s} = 0, (s = 1, 2), \quad (1.6)$$

$$\boldsymbol{\epsilon}_{\mathbf{k},s}^* \cdot \boldsymbol{\epsilon}_{\mathbf{k},s'} = \delta_{ss'} (s, s' = 1, 2), \quad (1.7)$$

$$\boldsymbol{\epsilon}_{\mathbf{k},1}^* \times \boldsymbol{\epsilon}_{\mathbf{k},2} = \frac{\mathbf{k}}{k} = \hat{\mathbf{k}}, \quad (1.8)$$

where eq. (1.6) means that the wave vector is orthogonal with each polarization vector, eq. (1.7) means that the polarization vectors are orthonormal and eq. (1.8) that the polarization vectors and wave vector form a right-handed triad [3].

For the sake of simplicity, we refer only to the first part of eq. (1.5). This part will be called positive-frequency electric field, and is given by

$$\begin{aligned} \mathbf{E}^+(r, t) &= \frac{i}{\epsilon_0^{1/2} L^{3/2}} \sum_{\mathbf{k}} \sum_s \omega_k [u_{\mathbf{k}s}(t) \boldsymbol{\epsilon}_{\mathbf{k},s} e^{i\mathbf{k}\cdot\mathbf{r}}] \\ &= \frac{i}{\epsilon_0^{1/2} L^{3/2}} \sum_{\mathbf{k}} \omega_k [u_{\mathbf{k}H}(t) \boldsymbol{\epsilon}_{\mathbf{k},H} e^{i\mathbf{k}\cdot\mathbf{r}} + u_{\mathbf{k}V}(t) \boldsymbol{\epsilon}_{\mathbf{k},V} e^{i\mathbf{k}\cdot\mathbf{r}}], \end{aligned} \quad (1.9)$$

where $\epsilon_{\mathbf{k},H}$, $\epsilon_{\mathbf{k},V}$ are the horizontal and vertical polarization vectors for each wave-vector \mathbf{k} . For paraxial beams, there is a predominancy of a propagation direction, parallel to some given \mathbf{k} , and the electric field is reduced to having only the components

$$\begin{aligned}\epsilon_H E_H^+(r, t) &= \frac{i}{\epsilon_0^{1/2} L^{3/2}} \sum_{\mathbf{k}} \omega_k u_{\mathbf{k}H}(t) \epsilon_{\mathbf{k},H} e^{i\mathbf{k}\cdot\mathbf{r}}, \\ \epsilon_V E_V^+(r, t) &= \frac{i}{\epsilon_0^{1/2} L^{3/2}} \sum_{\mathbf{k}} \omega_k u_{\mathbf{k}V}(t) \epsilon_{\mathbf{k},V} e^{i\mathbf{k}\cdot\mathbf{r}}.\end{aligned}\quad (1.10)$$

In the case of a laser beam, the frequency bandwidth is very narrow and only modes close to the axis of propagation should be taken into account giving the electric field

$$\mathbf{E}^+(r, t) = \epsilon_H E_H^+(r, t) + \epsilon_V E_V^+(r, t). \quad (1.11)$$

The vectors ϵ_H and ϵ_V conform an orthonormal basis, whose members are perpendicular to the propagation direction \mathbf{k} . They define a right handed triad. These basis vectors have a representation in a Hilbert space \mathcal{H}_2 . We can use Dirac notation and make the correspondence

$$\begin{aligned}\epsilon_H &\rightarrow |H\rangle \\ \epsilon_V &\rightarrow |V\rangle \\ \epsilon_D &\rightarrow \frac{1}{\sqrt{2}}(|H\rangle + |V\rangle) = |D\rangle \\ \epsilon_A &\rightarrow \frac{1}{\sqrt{2}}(|H\rangle - |V\rangle) = |A\rangle \\ \epsilon_R &\rightarrow \frac{1}{\sqrt{2}}(|H\rangle + i|V\rangle) = |R\rangle \\ \epsilon_L &\rightarrow \frac{1}{\sqrt{2}}(|H\rangle - i|V\rangle) = |L\rangle,\end{aligned}\quad (1.12)$$

where D/A refer to diagonal/antidiagonal polarization and R/L to right and left polarization. A general polarization state in Hilbert space \mathcal{H}_2 is given by

$$|\psi\rangle = \alpha |H\rangle + \beta |V\rangle, \quad (1.13)$$

where $\alpha, \beta \in \mathbb{C}$ and $\{|H\rangle, |V\rangle\}$ are the components for the orthonormal basis \mathcal{H}_2 . Similarly, we can express $|\psi\rangle$ in the other bases $\{|D\rangle, |A\rangle\}$ and $\{|R\rangle, |L\rangle\}$.

1.2.2 Path and polarization qubits

As it was mentioned in subsec. (1.2.1), two polarization vectors can be associated to a wave vector. Therefore, it is possible to use two wave vectors as two possible paths to form a path qubit. To illustrate this, we let the electric field being modified as it is shown below

$$\mathbf{E}^+(r, t) = \frac{i}{L^{3/2}} \sum_{\mathbf{k}} \left(\frac{\hbar\omega_{\mathbf{k}}}{2\epsilon_0} \right)^{1/2} [a_{\mathbf{k}H}(0)\boldsymbol{\epsilon}_{\mathbf{k},H}e^{i(\mathbf{k}\cdot\mathbf{r}-\omega t)} + a_{\mathbf{k}V}(0)\boldsymbol{\epsilon}_{\mathbf{k},V}e^{i(\mathbf{k}\cdot\mathbf{r}-\omega t)}], \quad (1.14)$$

where the mode amplitudes $u_{\mathbf{k}H}(0)$ and $u_{\mathbf{k}V}(0)$ are replaced by the operators $a_{\mathbf{k}H}(0)$ and $a_{\mathbf{k}V}(0)$, respectively.

For a general state with many paths, the Fock state with infinite occupation numbers is

$$|\{n\}\rangle = \prod_{\mathbf{k},s} |n_{\mathbf{k},s}\rangle, \quad (1.15)$$

where $|\{n\}\rangle$ represent all the set possibles of $n_{\mathbf{k},s}$.

Orthonormality is fulfilled in eq. (1.16)

$$\langle\{n\}|\{m\}\rangle = \prod_{\mathbf{k},s} \delta_{n_{\mathbf{k},s}m_{\mathbf{k},s}}. \quad (1.16)$$

This product represents propagation mode and polarization mode with \mathbf{k} and s , respectively, with the number of photons being n . Propagation and polarization modes are perpendicular, i.e., the two possible polarizations (s) are perpendicular to the propagation mode \mathbf{k} . The two states of polarization are orthogonal. The two states of polarization and mode of propagation form a right hand Cartesian basis.

An extensive form of eq. (1.15) for one photon state in the propagation \mathbf{k}_2 and polarization H

is

$$\dots |0_{\mathbf{k}_1, H}\rangle |0_{\mathbf{k}_1, V}\rangle |1_{\mathbf{k}_2, H}\rangle |0_{\mathbf{k}_2, V}\rangle |0_{\mathbf{k}_3, H}\rangle |0_{\mathbf{k}_3, H}\rangle \dots \quad (1.17)$$

It is more practical to reduce the expression for two orthogonal propagation modes \mathbf{k}_1 and \mathbf{k}_2 , given by

$$\begin{aligned} |\mathbf{k}_1, H\rangle &= \dots |1\rangle_{\mathbf{k}_1, H} |0\rangle_{\mathbf{k}_1, V} |0\rangle_{\mathbf{k}_2, H} |0\rangle_{\mathbf{k}_2, V} \dots, \\ |\mathbf{k}_2, H\rangle &= \dots |0\rangle_{\mathbf{k}_1, H} |0\rangle_{\mathbf{k}_1, V} |1\rangle_{\mathbf{k}_2, H} |0\rangle_{\mathbf{k}_2, V} \dots \end{aligned} \quad (1.18)$$

so that they read

$$\begin{aligned} |\mathbf{k}_1, H\rangle &\equiv |X, H\rangle \equiv |X\rangle \otimes |H\rangle, \\ |\mathbf{k}_2, H\rangle &\equiv |Y, H\rangle \equiv |Y\rangle \otimes |H\rangle, \end{aligned} \quad (1.19)$$

where $|X, H\rangle$ and $|Y, H\rangle$ are similarly defined, as perpendicular to one another. A general, path state is given by

$$|\psi\rangle = \alpha |X\rangle + \beta |Y\rangle, \quad (1.20)$$

where $\alpha, \beta \in \mathbb{C}$ and $\{|X\rangle, |Y\rangle\}$ is an orthonormal basis on Hilbert space \mathcal{H}_2 . In addition, it is possible to define a density matrix as it is done with polarization states, but our experiments were performed with pure path states.

1.3 Mixed states for polarization and path qubits

There is no pure state in nature. Real states are always an ensemble of many states, each one of its constituents entering with some probability. The uncertainty of the states comes from incomplete knowledge about the system and the representation of mixed states can be given

with density matrices. A mixed state is generally given by

$$\rho = \sum_i p_i \rho_i, \quad (1.21)$$

where $\rho_i = |\psi_i\rangle\langle\psi_i|$ is a pure state and p_i its probability. That is, pure states are combined incoherently in such way that the average of the states ρ_i with weights p_i results in ρ .

Given a two-state system $\{|H\rangle, |V\rangle\}$ in Hilbert space \mathcal{H}_2 , a general pure state $|\psi_i\rangle = c_{h,i}|H\rangle + \exp(i\phi_i)c_{v,i}|V\rangle$, whose coefficients $c_{h,i}, c_{v,i}$ are complex values, define the density matrix given by

$$\rho_i = \begin{pmatrix} |c_{h,i}|^2 & \exp(-i\phi_i)c_{h,i}c_{v,i}^* \\ \exp(i\phi_i)c_{h,i}^*c_{v,i} & |c_{v,i}|^2 \end{pmatrix}. \quad (1.22)$$

As an example, let us consider the case in which all states are identical, except for their phase distribution ϕ_i . The states can then be written as $|\psi_i\rangle = c_h|H\rangle + \exp(i\phi_i)c_v|V\rangle$ and their corresponding density matrices read

$$\rho_i = \begin{pmatrix} |c_h|^2 & \exp(-i\phi_i)c_h c_v^* \\ \exp(i\phi_i)c_h^* c_v & |c_v|^2 \end{pmatrix}. \quad (1.23)$$

If all the states occur with the same probability $p_i = 1/N$, where N is the number of states, the off diagonal elements of the total density matrix reduce to

$$\begin{aligned} \rho_{h,v} &= \sum_i p_i \exp(-i\phi_i) c_h c_v^* \\ &= c_h c_v^* \frac{1}{N} \sum_i \exp(-i\phi_i) \\ &= c_h c_v^* \frac{1}{2\pi} \int_0^{2\pi} \exp(-i\phi) d\phi \\ &= 0. \end{aligned} \quad (1.24)$$

It means that in mixed states the coherence between $|H\rangle$ and $|V\rangle$ cancels out [4], giving rise to a diagonal density matrix

$$\rho_i = \begin{pmatrix} |c_h|^2 & 0 \\ 0 & |c_v|^2 \end{pmatrix}, \quad (1.25)$$

which is the sum of two pure states $|H\rangle\langle H|$ and $|V\rangle\langle V|$, with probabilities $|c_h|^2$ and $|c_v|^2$, respectively.

In Sec. 1.1, we defined the geometric representation of a qubit. Replacing $\{|0\rangle, |1\rangle\}$ by $\{|H\rangle, |V\rangle\}$, a state can be represented on S^2 .

An arbitrary mixed state represents an ensemble of polarization states given by

$$\rho_M = \frac{\sigma_0 + \vec{s} \cdot \vec{\sigma}}{2}, \quad (1.26)$$

where $\sigma_0 = \mathbb{1}$, $\vec{s} = \left(\frac{\langle \hat{S}^{(1)} \rangle}{\langle \hat{S}_0 \rangle}, \frac{\langle \hat{S}_2 \rangle}{\langle \hat{S}_0 \rangle}, \frac{\langle \hat{S}_3 \rangle}{\langle \hat{S}_0 \rangle} \right)$ and $\vec{\sigma} = (\sigma_1, \sigma_2, \sigma_3)$ are the identity matrix, the Stokes vector and the Pauli matrices, respectively. The Stokes vector represents a vector on the Poincare sphere, plotted in Fig. 1.2, with length $|\vec{s}| \leq 1$ giving the degree of polarization, which is defined as $\mathcal{P} = \sqrt{\vec{s} \cdot \vec{s}}$.

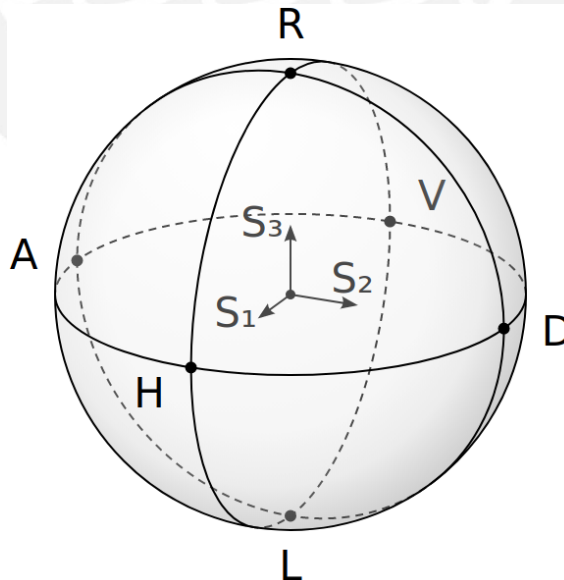


Figure 1.2: Poincare sphere.

The quantum Stokes vector operators are defined as follows:

$$\begin{aligned}
\hat{S}_0 &= a_H^\dagger a_H + a_V^\dagger a_V, \\
\hat{S}_1 &= a_H^\dagger a_H - a_V^\dagger a_V, \\
\hat{S}_2 &= a_D^\dagger a_D - a_A^\dagger a_A, \\
\hat{S}_3 &= a_R^\dagger a_R - a_L^\dagger a_L.
\end{aligned} \tag{1.27}$$

The mean values are

$$\begin{aligned}
s_1 &= \langle \hat{S}_1 \rangle / \langle \hat{S}_0 \rangle = \frac{\langle \hat{n}_H \rangle - \langle \hat{n}_V \rangle}{\langle \hat{n}_H \rangle + \langle \hat{n}_V \rangle}, \\
s_2 &= \langle \hat{S}_2 \rangle / \langle \hat{S}_0 \rangle = \frac{\langle \hat{n}_D \rangle - \langle \hat{n}_A \rangle}{\langle \hat{n}_H \rangle + \langle \hat{n}_V \rangle}, \\
s_3 &= \langle \hat{S}_3 \rangle / \langle \hat{S}_0 \rangle = \frac{\langle \hat{n}_R \rangle - \langle \hat{n}_L \rangle}{\langle \hat{n}_H \rangle + \langle \hat{n}_V \rangle}.
\end{aligned} \tag{1.28}$$

Some cases of degree of polarization will be related to a combination of states of $|H\rangle\langle H|$ and $|V\rangle\langle V|$. Some examples are the pure polarized state, the partially polarized state and the non-polarized state given by eq. (1.29), eq. (1.30) and eq. (1.31), respectively, as it is shown below

$$\rho = |V\rangle\langle V| \quad \vec{S} = (-1, 0, 0) \quad \mathcal{P} = 1, \tag{1.29}$$

$$\rho = \frac{3|H\rangle\langle H|}{4} + \frac{|V\rangle\langle V|}{4} \quad \vec{S} = (1/2, 0, 0) \quad \mathcal{P} = 1/2, \tag{1.30}$$

$$\rho = \frac{|H\rangle\langle H|}{2} + \frac{|V\rangle\langle V|}{2} \quad \vec{S} = (0, 0, 0) \quad \mathcal{P} = 0. \tag{1.31}$$

Likewise, for a path qubit it is possible to build a density matrix and define a sphere equivalent to Poincare sphere. However, it will be enough to deal with a pure state.

$$|\phi\rangle = \alpha |X\rangle + \beta |Y\rangle \tag{1.32}$$

$$\rho_S = |\phi\rangle\langle\phi|. \tag{1.33}$$

Finally, the most relevant properties for a mixed state are listed below

$$\begin{aligned}
 Tr(\rho) &= 1 \\
 \rho^\dagger &= \rho \\
 Tr(\rho^2) &\leq 1 \\
 \langle A \rangle &= Tr(A\rho) \\
 P_i &= Tr(|\psi_i\rangle\langle\psi_i| \rho).
 \end{aligned}
 \tag{1.34}$$

1.4 Extended polarization coherence theorem

According to Niels Bohr, the two views of light as wave or particle are limitations of a classical interpretation of experimental evidence of the nature of light[5]. Both the wave nature and the particle nature of light can be quantified with visibility (V) and distinguishability (D), respectively. Various authors derived the inequality (1.35) that establishes a constraint for the duality of the two behaviors of quantum light or any other quantum object (also called “quanta”) [6, 7, 8]:

$$V^2 + D^2 \leq 1. \tag{1.35}$$

A tight constraint for the duality behavior of quanta was derived and dubbed the polarization coherence theorem (PCT) [9]. The degree of polarization (P), which enters the PCT, is understood in its most general sense, which is a two-party property [9]. The constraint reads

$$V^2 + D^2 = P^2. \tag{1.36}$$

The term P should not be limited to light polarization, which is only a particular case. In general, it addresses all quantities that are susceptible of being “polarized”, such as propagation modes, spin, electric-field polarization, etc. The experimental evidence that supports eq. (1.36)

was carried out using classical light fields in a Mach-Zehnder interferometer[10]. Thereafter, an extended version of the PCT was given in [11]. In contrast to the PCT, that extension involves a path state and a polarization state, which acts as a marker in an interferometric scenario. The extension is given by

$$\mathcal{D}^2 + \mathcal{V}^2 = \cos^2 \frac{\gamma}{2} + \mathcal{P}^2 \sin^2 \frac{\gamma}{2}, \quad (1.37)$$

where the marker state undergoes a unitary evolution, which allows the distinction of one path from the other. The more efficient the marker is, the lower the capacity of the state to produce a well defined interference pattern.

The squared values of visibility and distinguishability can be shown to be given by [11]

$$\begin{aligned} \mathcal{V}^2 &= \cos^2 \frac{\gamma}{2} + \mathcal{P} \cos^2 \phi \sin^2 \frac{\gamma}{2}, \\ \mathcal{D}^2 &= \mathcal{P}^2 \sin^2 \phi \sin^2 \frac{\gamma}{2}, \end{aligned} \quad (1.38)$$

where γ is the angle rotated by the Stokes vector \vec{S} around the unit vector \hat{n} on the Poincare sphere. The latter vector is the rotation axis that is associated to the unitary operator acting on the polarization space. \mathcal{P} is the degree of polarization and ϕ is the angle between \vec{S} and \hat{n} . Experimental tests of this extension of the PCT have been conducted with classical light fields and a Mach-Zehnder type setup [12].

Chapter 2

Experimental arrangements

2.1 Generation of path states and mixed polarization states

2.1.1 Generation of path states

A beam submitted to a beam splitter gives rise to an output-state that is a superposition of two path states. Eq. (2.1) gives the unitary operator of a quantum beam splitter. It is given in terms of the two possible modes of propagation [13]:

$$S(\theta) = e^{i\theta(a_1^\dagger a_2 + a_2^\dagger a_1)}. \quad (2.1)$$

Here, a_1 and a_2 are the propagation modes and θ defines the amplitude coefficient for transmission and reflection. Photons are sent on mode 1 and the vacuum on mode 2, so that the evolution for a single photon is given by

$$|\text{out}\rangle = S |1_{\mathbf{k}_1}, 0_{\mathbf{k}_2}\rangle, \quad (2.2)$$

where $|1_{\mathbf{k}_1}, 0_{\mathbf{k}_2}\rangle$ represents the incoming photon. By introducing the identity operator and writing explicitly the creation operator of the incoming photon, the state becomes

$$\begin{aligned} |out\rangle &= Sa_1^\dagger S^\dagger S |0_{\mathbf{k}_1}, 0_{\mathbf{k}_2}\rangle \\ &= (a_1^\dagger \cos \theta + ia_2^\dagger \sin \theta) |0_{\mathbf{k}_1}, 0_{\mathbf{k}_2}\rangle. \end{aligned} \quad (2.3)$$

Eq. (2.3) results from $S |0_{\mathbf{k}_1}, 0_{\mathbf{k}_2}\rangle = |0_{\mathbf{k}_1}, 0_{\mathbf{k}_2}\rangle$ and $Sa_1^\dagger S^\dagger = a_1^\dagger \cos \theta + ia_2^\dagger \sin \theta$. For a symmetric beam splitter, which was used in our experimental setup, $\theta = \frac{\pi}{4}$. The final state is then

$$|out\rangle = \frac{1}{\sqrt{2}} [|1_{\mathbf{k}_1}, 0_{\mathbf{k}_2}\rangle + i |0_{\mathbf{k}_1}, 1_{\mathbf{k}_2}\rangle]. \quad (2.4)$$

The two states for single photon are $|1_{\mathbf{k}_1}, 0_{\mathbf{k}_2}\rangle$ and $|0_{\mathbf{k}_1}, 1_{\mathbf{k}_2}\rangle$. A two state system can be defined as two orthogonal states $\{|1\rangle, |2\rangle\}$ on \mathcal{H}_2 , with the following equivalence:

$$\begin{aligned} |1_{\mathbf{k}_1}, 0_{\mathbf{k}_2}\rangle &\equiv |1\rangle \\ |0_{\mathbf{k}_1}, 1_{\mathbf{k}_2}\rangle &\equiv |2\rangle. \end{aligned} \quad (2.5)$$

Hence, the output state after being submitted to a symmetric beam splitter is

$$|\phi\rangle = \frac{1}{\sqrt{2}} [|1\rangle + i |2\rangle] \quad (2.6)$$

or in the density matrix form

$$\rho_S = |\phi\rangle\langle\phi|, \quad (2.7)$$

which is a pure state in path space.

2.1.2 Generation of mixed polarization states

As for polarization space, a set of mixed polarized states is sent through a half-wave plate (HWP), which changes the vertical polarization to horizontal, in order that the weighting of

vertical and horizontal polarizations can be used to build a mixed state. Since visualization of polarizations states on the Poincare sphere will be used, it is necessary to describe the evolution of a state under the action of a birefringent plate. Elements of the unimodular and unitary group $SU(2)$ transform the polarization states and operate as single-qubit gates [14]. A subset of members of $SU(2)$, which depend on two parameters (instead of three), are given by

$$u_{(\zeta, \theta)} = e^{-i\frac{\zeta}{2}(\hat{n}(\theta) \cdot \boldsymbol{\sigma})}. \quad (2.8)$$

The unit vector $\hat{n} = (\cos 2\theta, \sin 2\theta, 0)$ lies on the $s_1 - s_2$ plane, ζ is the rotation angle around \hat{n} on the Poincare sphere and $\boldsymbol{\sigma} = (\sigma_1, \sigma_2, \sigma_3)$ is a vector of Pauli matrices. Eq. (2.8) for $\zeta = \pi$ and $\zeta = \pi/2$ can be realized by a half wave plate and quarter wave plate, respectively. For instance, given a vertical polarization, it is required to transform it into a horizontal polarization by a half wave plate. The value of $\theta = \frac{\pi}{4}$ and $\zeta = \pi$ on $u_{(\zeta, \theta)}$ realize this transformation. Eq. (2.9) represents that evolution:

$$|V\rangle\langle V| = u_{\pi, \frac{\pi}{4}} |H\rangle\langle H| u_{\pi, \frac{\pi}{4}}^\dagger. \quad (2.9)$$

Fig. 2.1 shows a scheme that allows to generate $|V\rangle$ states with adjustable weights.

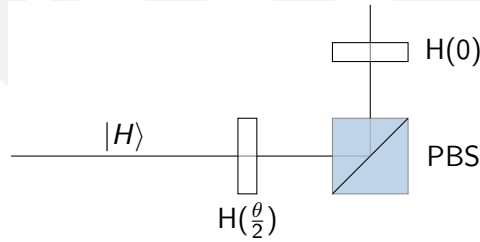


Figure 2.1: Scheme for generation of $|V\rangle$ state.

The generated state is $\sin \theta |V\rangle$.

Fig. 2.2 shows a scheme that allows to generate $|H\rangle$ states with adjustable weights.

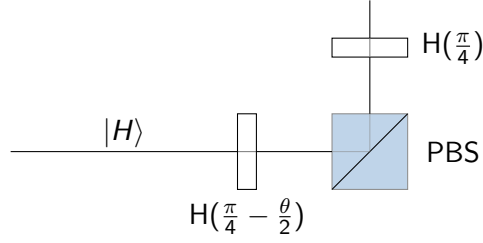


Figure 2.2: Scheme for generation of $|H\rangle$ state.

The generated state is $\cos \theta |H\rangle$.

For a two-state system $\{|H\rangle, |V\rangle\}$, the two polarized states can be produced incoherently, giving rise to three types of mixed polarizations: completely polarized, partially polarized and unpolarized. Eq. (2.10) gives a mixed state, an incoherent combination of $|H\rangle$ state and $|V\rangle$ states:

$$\rho_M = \cos^2 \theta |H\rangle\langle H| + \sin^2 \theta |V\rangle\langle V|. \quad (2.10)$$

As was seen in Sec. 1.3, the degree of polarization is given by $\mathcal{P} = \sqrt{\vec{s} \cdot \vec{s}} = \cos 2\theta$. If $\theta = \pi/2$ or $\theta = 0$, the state will be a completely polarized state, $\mathcal{P} = 1$. On the other hand, if $\theta = \pi/4$, the state will be an unpolarized state, $\mathcal{P} = 0$. All other states are partially polarized states. This method will be applied to build a mixed state on polarization space. Any kind of mixed states can be given by the equation

$$\rho_M = \frac{\sigma_0 + \vec{s} \cdot \vec{\sigma}}{2}. \quad (2.11)$$

2.2 Experimental setup

Following the definitions in Sec. 2.1 of path and polarization states, we consider the tensor product of a path state (the system) and a polarization state (the marker) given by

$$\rho_{S+M} = \rho_S \otimes \rho_M, \quad (2.12)$$

which is submitted to a unitary evolution, given by a beam-splitter and a half wave plate. This combination operates on both path and polarization spaces. The unitary evolution of the optical elements are defined by the eqs. (2.13) and (2.14), respectively:

$$U_{BS} = \frac{1}{\sqrt{2}}(\sigma_1 + \sigma_2), \quad (2.13)$$

$$H(\beta) = -i(\cos(2\beta)\sigma_1 + \sin(2\beta)\sigma_2). \quad (2.14)$$

We also consider unitary evolutions in polarization space. Each of them is applied on one arm of the interferometer and are given by $U_1 = H(\frac{\gamma}{8})$ and $U_2 = H(-\frac{\gamma}{8})$. The global unitary evolution of the system is

$$U_{SM} = \sigma^\dagger \sigma U_1 + \sigma \sigma^\dagger U_2 e^{i\delta}, \quad (2.15)$$

where $\sigma = |2\rangle\langle 1|$, $\sigma^\dagger = |1\rangle\langle 2|$, and $e^{i\delta}$ is a relative phase shift.

The evolution of the total system (SM) is given by

$$\begin{aligned} \rho_{SM} &= U_{SM}(\rho_S^{(0)} \otimes \rho_M^{(0)})U_{SM}^\dagger \\ &= |\alpha|^2 \sigma^\dagger \sigma \rho_M^{(1)} + |\beta|^2 \sigma \sigma^\dagger \rho_M^{(2)} + \alpha^* \beta \sigma e^{i\delta} \tilde{\rho}_M + \beta^* \alpha \sigma^\dagger e^{-i\delta} \tilde{\rho}_M^\dagger. \end{aligned} \quad (2.16)$$

Here, $\rho_M^{(k)} = U_k \rho_M^{(0)} U_k^\dagger$, $k = 1, 2$, and $\tilde{\rho}_M = U_2 \rho_M^{(0)} U_1^\dagger$.

The new path state is given by

$$\rho_S = \text{Tr}_M(\rho_{SM}) = |\alpha|^2 \sigma^\dagger \sigma + |\beta|^2 \sigma \sigma^\dagger + \alpha^* \beta e^{i\delta} \mathcal{C} \sigma + \alpha \beta^* e^{-i\delta} \mathcal{C}^* \sigma^\dagger, \quad (2.17)$$

where $\mathcal{C} = \text{Tr}_M(\tilde{\rho}_M)$.

Finally, the state S is submitted to a symmetric BS, resulting in

$$\rho_S^F = U_{BS} \rho_S U_{BS}^\dagger. \quad (2.18)$$

After measuring the intensity on the detector as it is shown in Fig. 2.3 , placed on one output of the interferometer, the results is

$$I^{(1)} = \text{Tr}(\sigma^\dagger \sigma \rho_S^F) = \frac{1}{2}[|\alpha|^2 + |\beta|^2 + 2\Re(\alpha\beta^* e^{i\delta} C)]. \quad (2.19)$$

Here, \Re means the real part of its argument.

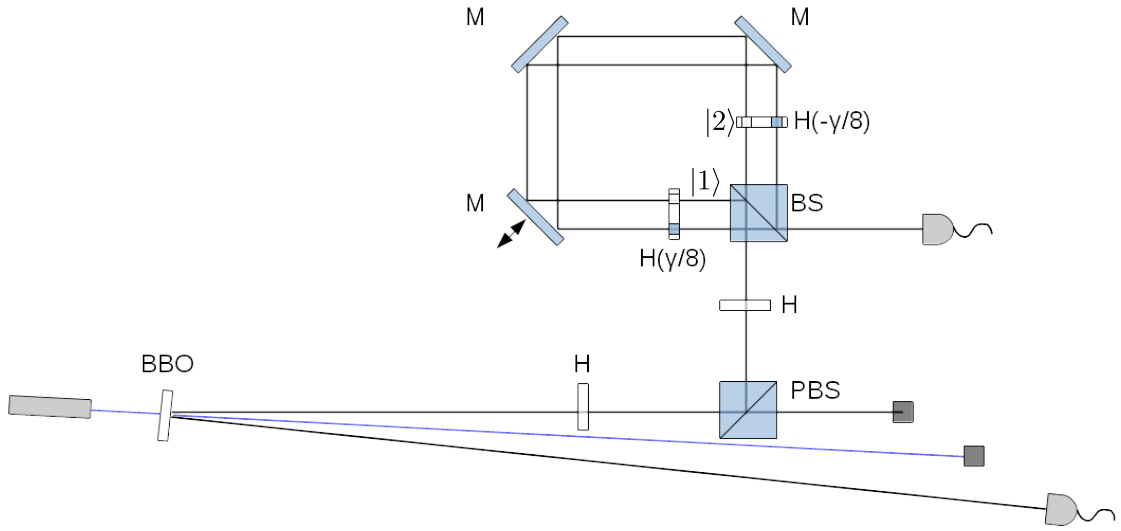


Figure 2.3: Sagnac-type interferometer.

For a symmetrical beam splitter at the beginning, $\rho_S^{(0)} = |\phi\rangle\langle\phi|$ with $|\phi\rangle = \frac{1}{\sqrt{2}}(|1\rangle + |2\rangle)$ give the intensity

$$I^{(1)} = [1 + |C| \cos(\delta + \arg C)]/2. \quad (2.20)$$

It can be shown that visibility equals the module of coherence (C):

$$\mathcal{V} = \frac{I_{max}^{(1)} - I_{min}^{(1)}}{I_{max}^{(1)} + I_{min}^{(1)}} = |C|. \quad (2.21)$$

As for distinguishability, we have that

$$\begin{aligned}\rho_M &= \text{Tr}_S(\rho_{SM}) = |\alpha|^2 \rho_M^{(1)} + |\beta|^2 \rho_M^{(2)}, \\ \mathcal{D} &= \text{Tr} \left| |\alpha|^2 \rho_M^{(1)} - |\beta|^2 \rho_M^{(2)} \right|.\end{aligned}\tag{2.22}$$

The last term can be simplified, because the initial path state we consider has the values $|\alpha| = |\beta| = \frac{1}{\sqrt{2}}$.

Finally, the visibility and distinguishability are given by

$$\mathcal{V} = |\text{Tr}_M \tilde{\rho}_M| \quad \mathcal{D} = \frac{1}{2} \text{Tr} \left| \rho_M^{(1)} - \rho_M^{(2)} \right|,\tag{2.23}$$

where $|A| = \sqrt{A^\dagger A}$, for an operator A . We have also $\rho_M^{(0)} = \frac{1}{2}(\sigma_0 + \mathbf{s} \cdot \boldsymbol{\sigma})$. The value of distinguishability is given by the trace distance between $\rho_M^{(1)}$ and $\rho_M^{(2)}$, which corresponds to the Euclidean distance between the Stokes vectors of each state:

$$\mathcal{D} = \frac{1}{2} \text{Tr} \left| \rho_M^{(1)} - \rho_M^{(2)} \right| = \frac{1}{2} |\mathbf{S}^{(1)} - \mathbf{S}^{(2)}|,\tag{2.24}$$

where $\mathbf{S}^{(1)} = \mathcal{R}_1 \mathbf{S}$ and $\mathbf{S}^{(2)} = \mathcal{R}_2 \mathbf{S}$ are the Stokes vectors after being submitted to the unitary evolutions U_1 and U_2 whose 3D rotation operators are \mathcal{R}_1 and \mathcal{R}_2 , respectively.

The Euler-Rodrigues parameters are defined by $e_0 = \cos(\frac{\gamma}{2})$ and $\hat{\mathbf{e}} = \sin(\frac{\gamma}{2}) \hat{\mathbf{n}}$. Parameters γ and $\hat{\mathbf{n}}$ define the rotation angle and the vector around which the Stokes vector rotates on the Poincare sphere, respectively. Therefore, the value of the squared distinguishability will be

$$\mathcal{D}^2 = \mathbf{e}^2 \mathbf{S}^2 - (\mathbf{e} \cdot \mathbf{S})^2.\tag{2.25}$$

As for squared visibility, it is given by

$$\mathcal{V}^2 = e_0^2 + (\mathbf{e} \cdot \mathbf{S})^2.\tag{2.26}$$

The final equation that constrains visibility and distinguishability is

$$\mathcal{V}^2 + \mathcal{D}^2 = \cos^2 \frac{\gamma}{2} + \mathcal{P}^2 \sin^2 \frac{\gamma}{2}, \quad (2.27)$$

where the individual expressions for visibility and distinguishability are

$$\mathcal{V}^2 = \cos^2 \frac{\gamma}{2} + \mathcal{P}^2 \cos^2 \phi \sin^2 \frac{\gamma}{2}, \quad (2.28)$$

$$\mathcal{D}^2 = \mathcal{P}^2 \sin^2 \phi \sin^2 \frac{\gamma}{2}. \quad (2.29)$$

The parameter \mathcal{P} is the degree of polarization, γ is the angle rotated by the Stokes vector \vec{S} around the unit vector \hat{n} , and ϕ is the angle between \vec{S} and \hat{n} .

2.3 Technical information and experimental details

2.3.1 Technical information

Technical details of the devices used in the experiment are given in what follows.

The diode laser we used was a 405 nm continuous-wave with spectral line-width between 0.5 and 1 nm and output power of 37.5 mW. The single photon source was a beta barium borate (BBO) crystal which produces twin photons of wavelength 810 nm. The twin photons were detected by two avalanche photodetectors within a 10.42 ns time window. The photon-counting module Perkin-Elmer SPCM-AQ4C counted the photons after converging lenses and multi-mode fiber-optic cables. Dichroic filters Thorlabs FB800-40, FWHM: 40 ± 8 nm centered at 800 ± 8 nm were used to filter spurious counts.

The degree of second order coherence $g^2(0)$ was the parameter used to distinguish between classical and quantum fields. A value $g^2(0) < 1$ indicates that the light is non-classical. The

measurement of $g^2(0)$ was made in the laboratory with the result $g^2(0) = 0.187 \pm 0.011$, in accordance with [15].

The half wave plate Thorlabs WPH05M-808 was mounted on Thorlabs RSP1/M rotation mounts, the beam splitter was a Thorlabs BS-014, the polarizing beam splitter was a Thorlabs PBS-252 and the mirror a Thorlabs BB1-E02.

2.3.2 Experimental details

It is worth to mention some experimental aspects that affected our measurements.

Imperfect beam splitter: Although the beam splitter used in the laboratory was supposed to divide the laser beam in two beams of equal intensity, the experimental data showed that the transmitted and reflected beams were not equally distributed, i.e., in 50:50 relation, but in 40:60. This affected the visibility, because an unbalanced interferometer reduces the contrast of the interference fringes.

Mirror phase: Theoretically, the reflection produces a relative phase of $\pi/2$ between the horizontal and vertical polarization states. This is a physical restriction to put on the unitary evolution devices, the HWPs. It was convenient to maintain the polarization state along the path without changes. Thus, the HWPs were placed at the end of the two possible paths, as shown in 2.3.

Phase between $|H\rangle$ and $|V\rangle$ states after the beam splitter: The beam splitter used in the laboratory, ideally, does not change the polarization, but the experimental data showed that for any polarization of a superposition of horizontal and vertical states there is an added phase in the vertical component. This phase made it impossible to have two perfect orthogonal polarizations, as it is evident in Figs. 3.2 and 3.3 for $\gamma = \pi$.

Imperfect alignment: An imperfect alignment does not allow a visibility close to the value of 1, as is plotted in Figs. 3.1, 3.2 and 3.3.

Polarizer for states $|H\rangle$ and $|V\rangle$: After generating $|H\rangle$ and $|V\rangle$, see Fig. 2.3, these states were not completely polarized but had a non-zero value in the third component of the Stokes vector which propagated an error in distinguishability and visibility. A polarizer could “clean” these states so as to be closer to the ideal state.



Chapter 3

Results

3.1 Measurement of visibility

As mentioned in Sec. 2.2, the value of \mathcal{V}^2 depends on three parameters: γ , ϕ and \mathcal{P} . The first one is the rotated angle around the axis \hat{n} of the Stokes vector \vec{S} . The second one is the angle between \hat{n} and \vec{S} , which equals $\phi = \frac{\pi}{2}$ because \vec{S} is on the plane $s_1 - s_2$ and \hat{n} lies along the s_3 axis. The last parameter, \mathcal{P} , is the degree of polarization. The states are completely polarized, partially polarized and non polarized with the values $\mathcal{P} = 1$, $\mathcal{P} = 0.5$ and $\mathcal{P} = 0$, respectively. As was seen in Sec. 2.2, the visibility is the normalized difference between the maximum and minimum intensities. For non-classical light, the number of photons n is used instead of intensity, giving the result

$$\mathcal{V}(\gamma) = \frac{n_{max} - n_{min}}{n_{max} + n_{min}}, \quad (3.1)$$

where

$$n = n_H + n_V \quad (3.2)$$

and n_H and n_V are labels that refer, respectively, to the number of counts of H -polarized states and the number of counts of V -polarized states, which as components of the mixed state, are

submitted to the interferometer and then measured. Hence, the fraction of horizontal and vertical photon counts are eqs. (3.3) and (3.4), respectively:

$$n_H = \frac{\cos^2 \theta}{2} \left(1 + \cos \frac{\gamma}{2} \cos \delta\right), \quad (3.3)$$

$$n_V = \frac{\sin^2 \theta}{2} \left(1 + \cos \frac{\gamma}{2} \cos \delta\right), \quad (3.4)$$

$$n = \frac{1}{2} \left(1 + \cos \frac{\gamma}{2} \cos \delta\right) = n_H + n_V. \quad (3.5)$$

In the next three subsections, the measurement of the squared visibility in Figs. 3.1, 3.2 and 3.3 show three different behaviors of light: the wave-like and the particle-like behavior, plus an intermediate case, which corresponds neither to wave nor to particle. For all mentioned figures, the interferometer with HWPs set to $\gamma = 0$ or $\gamma = 2\pi$ reduces the capability of distinguishing whether a photon went along one path or the other. This feature corresponds to a wave behavior. In contrast, the value $\gamma = \pi$ distinguishes completely the two paths. Thus, the two possible, orthogonal polarizations give information of the path along which the photon went. An intermediate case is any value of $\{\gamma \in [0, 2\pi], \gamma \neq \{0, \pi, 2\pi\}\}$ which means that partial information of the photon path corresponds to a behavior that changes from wave-like to particle-like through intermediate cases.

3.1.1 Pure polarized states

A pure state has the degree of polarization $\mathcal{P} = 1$, which means that $\theta = 0$. Thus, the polarization state is

$$\rho_M^{(0)} = |H\rangle\langle H|, \quad (3.6)$$

where the superscript (0) refers to the preparation state, i.e., the state before entering the interferometer. The number of photon counts at the output is

$$n = n_H = \frac{1}{2} \left(1 + \cos \frac{\gamma}{2} \cos \delta \right). \quad (3.7)$$

The visibility function is given by

$$\mathcal{V}(\gamma) = \frac{n_{H,max} - n_{H,min}}{n_{H,max} + n_{H,min}} \quad (3.8)$$

and its square is plotted by

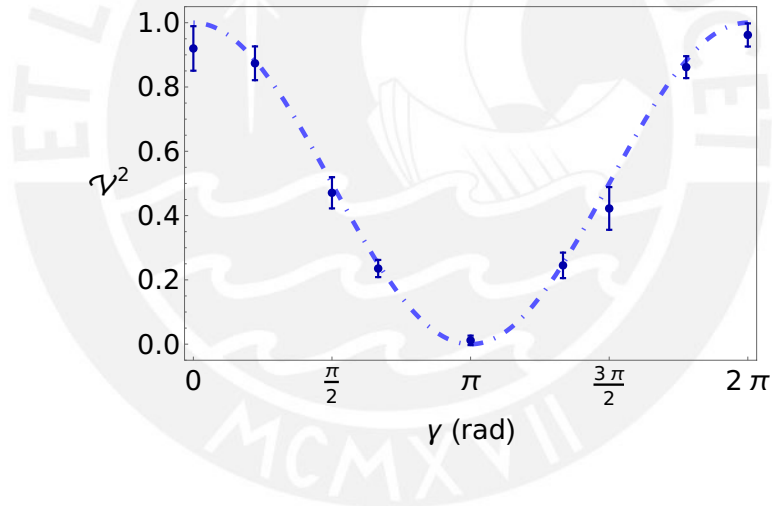


Figure 3.1: \mathcal{V}^2 for $\mathcal{P} = 1$.

3.1.2 Partially polarized states

For addressing partially polarized states, the degree of polarization chosen was $\mathcal{P} = 1/2$, which means that the value of $\theta = \pi/6$. Thus, the polarization state is

$$\rho_M^{(0)} = \frac{3|H\rangle\langle H|}{4} + \frac{|V\rangle\langle V|}{4}. \quad (3.9)$$

The output number of photon counts is

$$n = n_H + n_V = \frac{1}{2}(1 + \cos \frac{\gamma}{2} \cos \delta). \quad (3.10)$$

It is possible to express the number of counts of horizontal and vertical polarization states with eqs. (3.3) and (3.4), respectively. The results are

$$n_H = \frac{3}{8}(1 + \cos \frac{\gamma}{2} \cos \delta), \quad (3.11)$$

$$n_V = \frac{1}{8}(1 + \cos \frac{\gamma}{2} \cos \delta). \quad (3.12)$$

The visibility function is given by

$$\mathcal{V}(\gamma) = \frac{n_{H,max} + n_{V,max} - n_{H,min} - n_{V,min}}{n_{H,max} + n_{V,max} + n_{H,min} + n_{V,min}} \quad (3.13)$$

and its square is plotted below

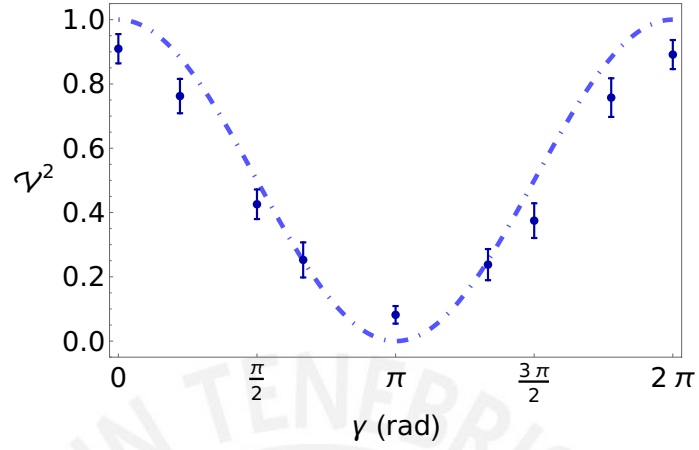


Figure 3.2: \mathcal{V}^2 for $\mathcal{P} = 0.5$.

3.1.3 Non polarized states

For a completely unpolarized state, the degree of polarization is $\mathcal{P} = 0$ which means that $\theta = \pi/4$. The polarization state is

$$\rho_M^{(0)} = \frac{|H\rangle\langle H|}{2} + \frac{|V\rangle\langle V|}{2}. \quad (3.14)$$

The output number of counts is

$$n = n_H + n_V = \frac{1}{2}(1 + \cos \frac{\gamma}{2} \cos \delta). \quad (3.15)$$

It is possible to express the number of counts of horizontal and vertical polarization states with eqs. (3.3) and (3.4), respectively. The results are

$$n_H = \frac{1}{4}(1 + \cos \frac{\gamma}{2} \cos \delta) \quad (3.16)$$

$$n_V = \frac{1}{4}(1 + \cos \frac{\gamma}{2} \cos \delta). \quad (3.17)$$

The visibility function is given by

$$\mathcal{V}(\gamma) = \frac{n_{H,max} + n_{V,max} - n_{H,min} - n_{V,min}}{n_{H,max} + n_{V,max} + n_{H,min} + n_{V,min}} \quad (3.18)$$

and its square is plotted below

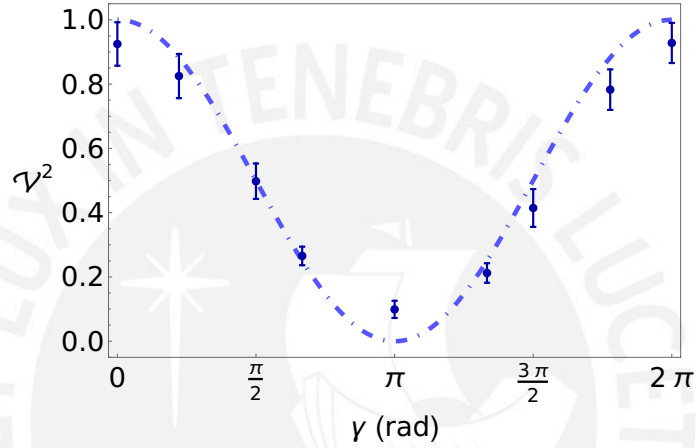


Figure 3.3: \mathcal{V}^2 for $\mathcal{P} = 0$.

3.2 Measurement of distinguishability

For a symmetric beam splitter, the distinguishability is

$$\mathcal{D} = \frac{1}{2} \text{Tr} \left| \rho_M^{(1)} - \rho_M^{(2)} \right|. \quad (3.19)$$

The equivalent value, in terms of Stokes vectors, is given by

$$\mathcal{D} = \frac{1}{2} |\mathbf{S}^{(1)} - \mathbf{S}^{(2)}|. \quad (3.20)$$

The measurement of $\mathbf{S}^{(1)}$ and $\mathbf{S}^{(2)}$ were made possible by blocking the transmitted and reflected paths in Fig. 3.4. Polarization tomography was made by using a QWP, HWP and a polarizer. The six projections of polarization states, mentioned in Sec. 1.3, were made by setting the following set of angles

$$\begin{aligned}
 n_H &= \left(P(\pi/2)H(\pi/4)Q(0) \right) \rho \left(P(\pi/2)H(\pi/4)Q(0) \right)^\dagger, \\
 n_V &= \left(P(\pi/2)H(0)Q(0) \right) \rho \left(P(\pi/2)H(0)Q(0) \right)^\dagger, \\
 n_D &= \left(P(\pi/2)H(-\pi/8)Q(\pi/4) \right) \rho \left(P(\pi/2)H(-\pi/8)Q(\pi/4) \right)^\dagger, \\
 n_A &= \left(P(\pi/2)H(\pi/8)Q(\pi/4) \right) \rho \left(P(\pi/2)H(\pi/8)Q(\pi/4) \right)^\dagger, \\
 n_R &= \left(P(\pi/2)H(\pi/8)Q(0) \right) \rho \left(P(\pi/2)H(\pi/8)Q(0) \right)^\dagger, \\
 n_L &= \left(P(\pi/2)H(-\pi/8)Q(0) \right) \rho \left(P(\pi/2)H(-\pi/8)Q(0) \right)^\dagger.
 \end{aligned} \tag{3.21}$$

These projections allowed to determine the Stokes vectors $\mathbf{S}^{(1)}$ and $\mathbf{S}^{(2)}$. As shown in eq. (2.29), the distinguishability depends on \mathcal{P} and γ .

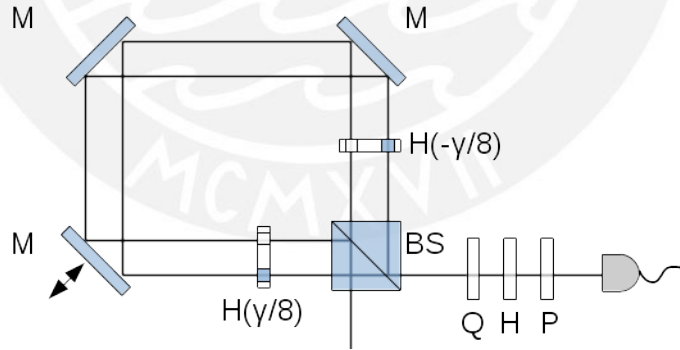


Figure 3.4: Tomography of stokes vector

Similarly to the previous Sec. 3.1, three cases for the degree of polarization can be addressed: pure polarized states, partially polarized states and non-polarized states. The measurement of the squared distinguishability in Figs. 3.5 and 3.6 show three aspects of complementary behavior of the squared visibility: the completely wave-like, particle-like and an intermediate value

which is neither wave nor particle. As can be seen in the mentioned figures, the interferometer with HWPs set to $\gamma = 0$ or $\gamma = 2\pi$ reduces the capability of distinguishing if one photon went to one path or the other. This feature is proper of a wave behavior. The distinguishability is at the minimum possible: $\mathcal{D}^2 = 0$. In contrast, the value $\gamma = \pi$ lets distinguish the two paths, giving a sharpened or degraded quality of \mathcal{D}^2 , depending on the degree of polarization. The values $\mathcal{P} = 1$ and $\mathcal{P} = 0.5$ correspond to a particle behavior and the distinguishabilities are at their maximum possible values $\mathcal{D}^2 = 1$ and $\mathcal{D}^2 = 0.25$, respectively. Thus, the degree of polarization regulates information of the path along which the photon went. An intermediate case corresponds to values $\{\gamma \in [0, 2\pi], \gamma \neq \{0, \pi, 2\pi\}\}$ which emphasizes that a partial information of the knowledge of the path of the photon can lead the behavior from wave-like to particle-like through intermediate cases.

Contrary to the results in Figs. 3.5 and 3.6 the measurement of distinguishability in Fig. 3.7 remains constant along the range of γ because of the value of the degree of polarization $\mathcal{P} = 0$. The capability of distinguishing one path-state from the other is always 0, despite the evolution of the polarization states. Thus, it is possible to say that there is no information to know which path the photon passed through.

3.2.1 Pure polarized states

For a pure state, the degree of polarization is $\mathcal{P} = 1$. Thus, the polarization state is

$$\rho_M^{(0)} = |H\rangle\langle H|. \quad (3.22)$$

Its evolution is given by

$$\rho_M^{(i)} = U_i |H\rangle\langle H| U_i^\dagger; \quad i = 1, 2. \quad (3.23)$$

Therefore, the Stokes vector is

$$\begin{aligned}\text{Tr}(\boldsymbol{\sigma}\rho_M^{(i)}) &= \text{Tr}(\boldsymbol{\sigma}U_i|H\rangle\langle H|U_i^\dagger) \\ \mathbf{S}^{(i)}(\gamma) &= \mathbf{S}_H^{(i)}(\gamma),\end{aligned}\tag{3.24}$$

where the subscript in $S_H^{(i)}$ refers to the initial polarization. The two Stokes vectors $\mathbf{S}^{(1)}$ and $\mathbf{S}^{(2)}$ are

$$\mathbf{S}^{(1)}(\gamma) = \mathbf{S}_H^{(1)}(\gamma)\tag{3.25}$$

$$\mathbf{S}^{(2)}(\gamma) = \mathbf{S}_H^{(2)}(\gamma).\tag{3.26}$$

Thus, the distinguishability is given by

$$\mathcal{D}(\gamma) = \frac{1}{2}|\mathbf{S}_H^{(1)}(\gamma) - \mathbf{S}_H^{(2)}(\gamma)|.\tag{3.27}$$

and its square is plotted below

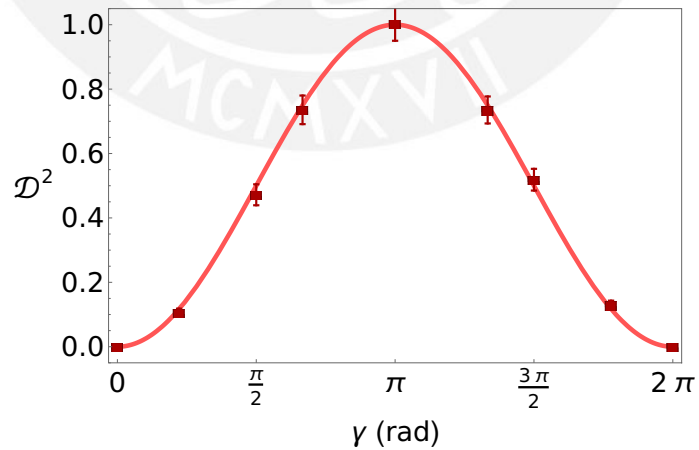


Figure 3.5: \mathcal{D}^2 for $\mathcal{P} = 1$.

3.2.2 Partially polarized state

We considered a partially polarized state, whose degree of polarization was $\mathcal{P} = 0.5$. Thus, the state was given by

$$\rho_M^{(0)} = \frac{3}{4} |H\rangle\langle H| + \frac{1}{4} |V\rangle\langle V|. \quad (3.28)$$

Its evolution is

$$\rho_M^{(i)} = \frac{3}{4} U_i |H\rangle\langle H| U_i^\dagger + \frac{1}{4} U_i |V\rangle\langle V| U_i^\dagger; \quad i = 1, 2. \quad (3.29)$$

Therefore, the Stokes vector is

$$\text{Tr}(\boldsymbol{\sigma} \rho_M^{(i)}) = \frac{3}{4} \text{Tr}(\boldsymbol{\sigma} U_i |H\rangle\langle H| U_i^\dagger) + \frac{1}{4} \text{Tr}(\boldsymbol{\sigma} U_i |V\rangle\langle V| U_i^\dagger) \quad (3.30)$$

$$\mathbf{S}^{(i)}(\gamma) = \mathbf{S}_H^{(i)}(\gamma) + \mathbf{S}_V^{(i)}(\gamma). \quad (3.31)$$

The two Stokes vectors $\mathbf{S}^{(1)}$ and $\mathbf{S}^{(2)}$ are given in eqs. (3.32) and (3.33), respectively:

$$\mathbf{S}^{(1)}(\gamma) = \mathbf{S}_H^{(1)}(\gamma) + \mathbf{S}_V^{(1)}(\gamma) \quad (3.32)$$

$$\mathbf{S}^{(2)}(\gamma) = \mathbf{S}_H^{(2)}(\gamma) + \mathbf{S}_V^{(2)}(\gamma). \quad (3.33)$$

The distinguishability is given by

$$\mathcal{D}(\gamma) = \frac{1}{2} \left| \mathbf{S}_H^{(1)}(\gamma) + \mathbf{S}_V^{(1)}(\gamma) - \mathbf{S}_H^{(2)}(\gamma) - \mathbf{S}_V^{(2)}(\gamma) \right| \quad (3.34)$$

and its square is plotted below

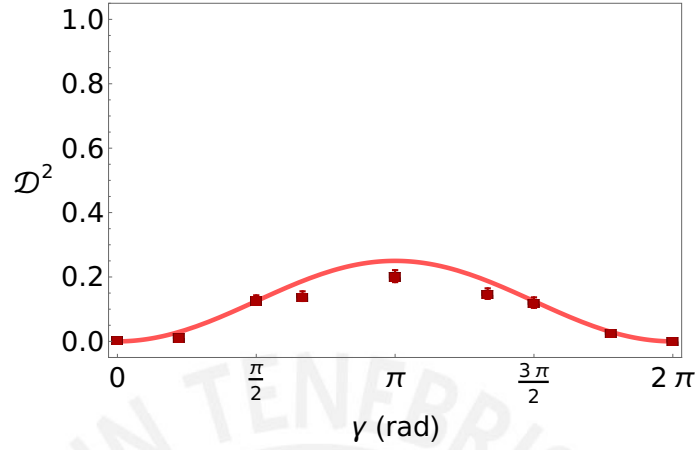


Figure 3.6: \mathcal{D}^2 for $\mathcal{P} = 0.5$.

3.2.3 Non polarized state

A non polarized state has the degree of polarization $\mathcal{P} = 0$. Thus, the state is

$$\rho_M^{(0)} = \frac{1}{2} |H\rangle\langle H| + \frac{1}{2} |V\rangle\langle V|. \quad (3.35)$$

Its evolution is

$$\rho_M^{(i)} = \frac{1}{2} U_i |H\rangle\langle H| U_i^\dagger + \frac{1}{2} U_i |V\rangle\langle V| U_i^\dagger; \quad i = 1, 2. \quad (3.36)$$

Therefore, the Stokes vector is

$$\text{Tr}(\boldsymbol{\sigma} \rho_M^{(i)}) = \frac{1}{2} \text{Tr}(\boldsymbol{\sigma} U_i |H\rangle\langle H| U_i^\dagger) + \frac{1}{2} \text{Tr}(\boldsymbol{\sigma} U_i |V\rangle\langle V| U_i^\dagger) \quad (3.37)$$

$$\mathbf{S}^{(i)}(\gamma) = \mathbf{S}_H^{(i)}(\gamma) + \mathbf{S}_V^{(i)}(\gamma). \quad (3.38)$$

The two Stokes vectors $\mathbf{S}^{(1)}$ and $\mathbf{S}^{(2)}$ are given by eqs. (3.39) and (3.40), respectively:

$$\mathbf{S}^{(1)}(\gamma) = \mathbf{S}_H^{(1)}(\gamma) + \mathbf{S}_V^{(1)}(\gamma) \quad (3.39)$$

$$\mathbf{S}^{(2)}(\gamma) = \mathbf{S}_H^{(2)}(\gamma) + \mathbf{S}_V^{(2)}(\gamma). \quad (3.40)$$

The distinguishability is given by

$$\mathcal{D}(\gamma) = \frac{1}{2} \left| \mathbf{S}_H^{(1)}(\gamma) + \mathbf{S}_V^{(1)}(\gamma) - \mathbf{S}_H^{(2)}(\gamma) - \mathbf{S}_V^{(2)}(\gamma) \right|. \quad (3.41)$$

and its square is plotted below

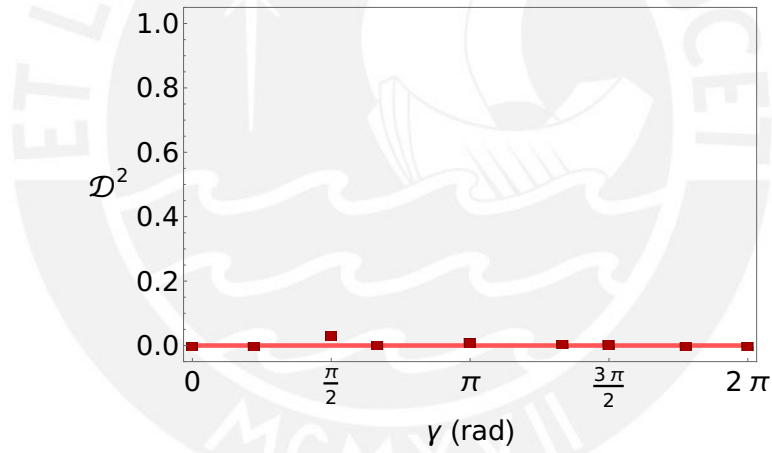


Figure 3.7: \mathcal{D}^2 for $\mathcal{P} = 0$.

3.3 The sum of visibility and distinguishability squared

The measurement of visibility, for the fixed angle $\phi = \pi/2$ is the result of varying the marker state which allows to make a distinction of the paths of the photon. It is revealed in the completely waveness behaviour with $\mathcal{V}^2 = 1$ or the particleness of the photon with $\mathcal{V}^2 = 0$. As

complementary behaviour of visibility is the calculation of distinguishability which is not only restricted to the evolution of the marker state but also to the type of the mixed state. This is the reason of the partial complementary behaviour with visibility because distinguishability depends on the marker evolution and the degree of polarization. As was mentioned in Secs. 3.1 and 3.2, a description of the duality behaviour of light is given by the sum $\mathcal{V}^2 + \mathcal{D}^2$.

3.3.1 Pure polarized state

For this state the evolution of the marker shows the complementary behaviour of visibility and distinguishability. According to the Fig. 3.8, the value of $\gamma = 0$ or $\gamma = 2\pi$ does not distinguish the path of the photon, then the wavelike behaviour is maximum $\mathcal{V}^2 = 1$ and distinguishability is at its lowest: $\mathcal{D}^2 = 0$. By contrast, the value of $\gamma = \pi$ distinguishes completely the path, then the wavelike behaviour is at its minimum $\mathcal{V}^2 = 0$ and the distinguishability is at its maximum: $\mathcal{D}^2 = 1$. An intermediate case corresponds to any value of $\{\gamma \in [0, 2\pi] | \gamma \neq \{0, \pi, 2\pi\}\}$ which emphasizes that partial information of the photon's path can lead the behaviour from wavelike to a partial particle-like through intermediate cases. As it is obvious, the sum $\mathcal{V}^2 + \mathcal{D}^2$ always is 1 in the range $\gamma \in [0, 2\pi]$.

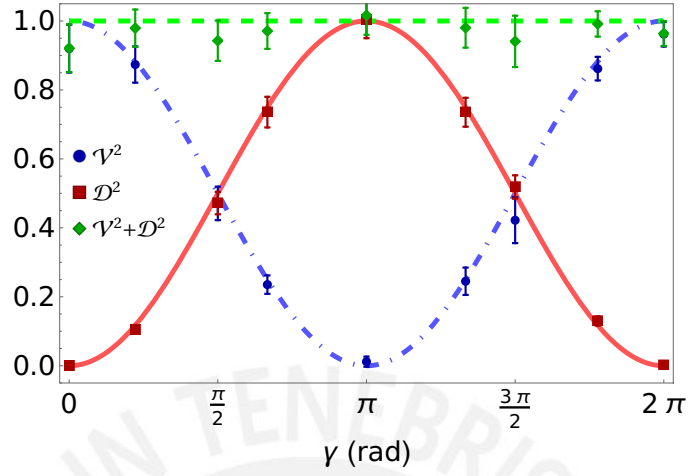


Figure 3.8: Plot of $\mathcal{V}^2 + \mathcal{D}^2$ for $\mathcal{P} = 1$.

3.3.2 Partially polarized state

For this state not only the evolution of the marker shows the complementary behaviour of visibility and distinguishability but also the degree of polarization which reduces the maximum value of the distinguishability. As shown in Fig. 3.9, the value of $\gamma = 0$ or $\gamma = 2\pi$ does not distinguish the path of the photon, then the wavelike behaviour is maximal $\mathcal{V}^2 = 1$ but the distinguishability is at its minimum: $\mathcal{D}^2 = 0$. By contrast, the value of $\gamma = \pi$ distinguishes partially the paths, then the distinguishability is the maximum possible given by the degree of polarization $\mathcal{D}^2 = 0.25$ and the visibility is minimum $\mathcal{V}^2 = 0$. As can be seen, the sum $\mathcal{V}^2 + \mathcal{D}^2$ is less than or equal to 1 in the range $\gamma \in [0, 2\pi]$ because of the reduction of distinguishability.

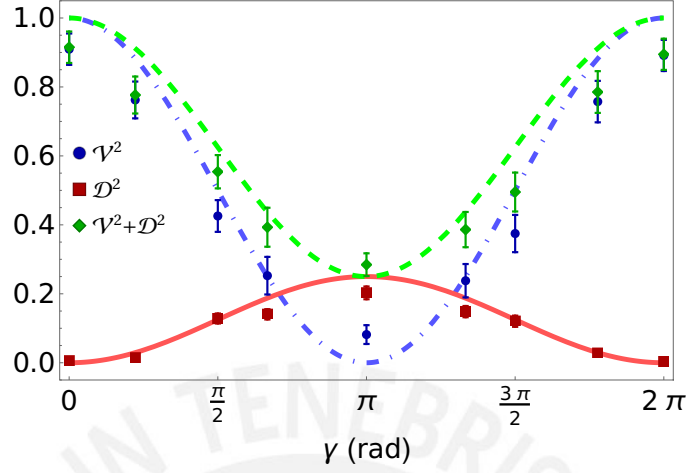


Figure 3.9: Plot of $\mathcal{V}^2 + \mathcal{D}^2$ for $\mathcal{P} = 0.5$.

3.3.3 Non polarized state

For this state the evolution of the marker only affects the visibility but not the distinguishability $\mathcal{D}^2 = 0$. In spite of the unitary evolution of the polarization state, there is no distinction between the transmitted and the reflected path states because of the degree of polarization. The visibility, in contraposition, maintains the feature of changing the behaviour from wavelike to particle-like. According to Fig. 3.10, the value of $\gamma = 0$ (or $\gamma = 2\pi$) does not distinguish the path of the photon, then the wavelike feature is at its maximum: $\mathcal{V}^2 = 1$, and the distinguishability is at its minimum: $\mathcal{D}^2 = 0$. In addition, for $\gamma = \pi$, the visibility is at its minimum: $\mathcal{V}^2 = 0$ and distinguishability remains constant, with $\mathcal{D}^2 = 0$. As it is clear, the sum $\mathcal{V}^2 + \mathcal{D}^2$ is always \mathcal{V}^2 in the range $\gamma \in [0, 2\pi]$.

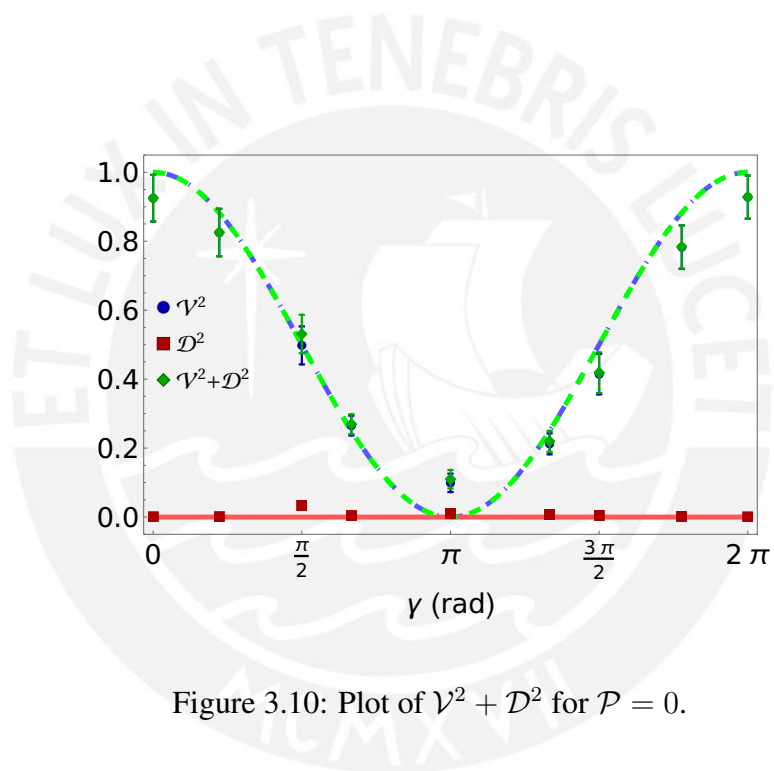


Figure 3.10: Plot of $\mathcal{V}^2 + \mathcal{D}^2$ for $\mathcal{P} = 0$.

Chapter 4

Summary

This thesis addressed several topics. In chapter 1, the analysis of a two-state system as a basic description of quantum effects allows introducing quantum bits as a useful tool to work in quantum and classical optics. Thereafter, the quantization of electromagnetic field played an important role to elucidate the nature of light revealed on the propagation of modes and the polarization states associated with any possible mode. Thus, any mode of propagation is a system of two degrees of freedom, the first is the mode of propagation along two possible paths and the second one is the polarization state. The background of the nature of light is a source for a more complex description of polarization as the statistical mixture of states. The definitions of mixed states of polarization and path state are degrees of freedom which are included in the extension of the polarization coherence theorem where the polarization works as a marker to change the behaviour of photons from waveness to particleness.

In the chapter 2, the experiment focuses on two parts, the generation of polarization mixed states and the evolution of the states. The first one is detailed in the generation of two orthogonal polarizations which will be joined to work with mixed states. These states were submitted to a unitary evolutions which operated on the marker state to distinguish the paths of the photon. The second part of the experimental setup is the sending of the mixed state in the sagnac interferometer to evolve and then interfere.

Finally, in the chapter 3, the measurements of visibility as a result of maximum counts and a minimum counts were made for three degree of polarization: pure polarized state, partially polarized state and non polarized state. By the other side, the measurement of distinguishability was made by tomography of stokes vectors of the transmitted path and reflected path. Therefore, the visibility squared plus the distinguishability squared verify the validation of polarization coherence theorem with photons. This experiment can be useful to extensions as a mixed path state and pure polarized state or including a general unitary evolution in the polarization space.



Bibliography

- [1] Hansen Vagn Lundsgaard. *Functional analysis*. World Scientific, 2006.
- [2] M.A. Nielsen and I.L. Chuang. *Quantum Computation and Quantum Information*. Cambridge University Press, 2010.
- [3] L. Mandel and E. Wolf. *Optical coherence and quantum optics*. Cambridge University Press, 1995.
- [4] M.O. Sargent III, M. Scully and W.E Lamb Jr. *Laser physics*. Addison-Wesley, 1974.
- [5] N. BOHR. The quantum postulate and the recent development of atomic theory1. *Nature*, 121(3050):580–590, Apr 1928.
- [6] Berthold-Georg Englert. Fringe visibility and which-way information: An inequality. *Phys. Rev. Lett.*, 77:2154–2157, Sep 1996.
- [7] X.-F. Qian, A. N. Vamivakas, and J. H. Eberly. Entanglement limits duality and vice versa. *Optica*, 5(8):942–947, Aug 2018.
- [8] Gregg Jaeger, Abner Shimony, and Lev Vaidman. Two interferometric complementarities. *Phys. Rev. A*, 51:54–67, Jan 1995.
- [9] J. H. Eberly, X.-F. Qian, and A. N. Vamivakas. Polarization coherence theorem. *Optica*, 4(9):1113–1114, Sep 2017.

- [10] Bhaskar Kanseri and Sethuraj K. R. Experimental observation of the polarization coherence theorem. *Opt. Lett.*, 44(1):159–162, Jan 2019.
- [11] F. De Zela. Hidden coherences and two-state systems. *Optica*, 5(3):243–250, Mar 2018.
- [12] P. Sánchez, J. Gonzales, V. Avalos, F. Auccapuclla, E. Suarez, and F. De Zela. Experimental display of the extended polarization coherence theorem. *Opt. Lett.*, 44(4):1052–1055, Feb 2019.
- [13] Christopher Gerry and Peter Knight. *Introductory Quantum Optics*. Cambridge University Press, 2004.
- [14] B. Neethi Simon, C. M. Chandrashekar, and Sudhavathani Simon. Hamilton’s turns as a visual tool kit for designing single-qubit unitary gates. *Phys. Rev. A*, 85:022323, Feb 2012.
- [15] Diego Eduardo Barberena Helfer. Geometric phases in polarization mixed states. Master’s thesis, Pontificia Universidad Católica del Perú, 2016.